



P-354

Detection of gas in sandstone reservoirs using AVO analysis in Cambay Basin. A case study.

B.M.Bhardwaj, C.V. Jambhekar , M.C.Kandpal, ONGC*

Summary

In this study, amplitude variation with offset (AVO) analysis was applied to the model from a well in the gas charged reservoir zone. AVO attributes, intercepts and gradient were calculated based on Aki-Richard's two term equation. Seismic data was reprocessed for better S/N ratio and by preserving relative amplitudes. Stretching and squeezing was applied to sonic log to generate good correlation between synthetic and seismic. Velocity model thus obtained was used for converting offset gathers to angle gathers. Synthetic angle gathers were compared with real PSTM gathers at well location for variation of amplitude with offset. Reversal of phase at the far offset was observed. AVO inversion was applied to seismic gathers to obtain intercept and gradient volumes. Cluster of AVO anomaly was identified from cross-plot of intercepts and gradient and was superimposed on intercepts section to bring out locales of AVO anomalies which provided lead for exploration of hydrocarbon in the area.

Keywords: Reflection amplitude, Hydrocarbon rock physics, Amplitude versus Offset attributes.

Introduction

The area under study is located in Cambay basin. Recently drilled exploratory wells have flowed gas and condensate from sandstone reservoir of Hazad Formation. This area is covered by 2D seismic data. Reservoir is high impedance and the seismic inversion could not provide much information about reservoir extent & quality. Amplitude versus offset (AVO) technique was therefore used to model subsurface synthetic response which was applied as seismic tool to avoid the ambiguity in interpretation and also as a direct technique to identify natural gas reservoir. AVO modeling was carried out in the target zone using rock properties obtained from log data and Aki-Richards equation. AVO anomaly classified as class II anomaly as per Rutherford and William classification where reflection coefficient was marginal positive near zero offset but change to highly negative at far offset. Synthetic angle gathers were created using AVO forward model which showed similar response as observed on real PSTM gathers for variation of amplitude with offset and phase reversal at far offsets/angles. AVO attributes created from seismic gathers i.e., Intercept and Gradient, were cross-plotted to identify the anomaly from background trend. This AVO

anomaly was superimposed on intercept section which helped to identifying prospective area for hydrocarbon exploration. One such representative AVO analysis / study limited to well-R and the seismic line b-b' passing through it is presented here.

Methodology

AVO technique is used to model subsurface synthetic response and as a direct technique to identify natural gas reservoirs. AVO analysis as seismic exploration tool is used to investigate dependence of seismic amplitudes on offset distance. Dependence of Seismic reflection energy upon interface reflection coefficient, angle of incidence and elastic parameters of medium was first studied by Knott (1899) than by Zeppritz (1919). Since the solution of the Zeppritz's matrix equations includes several unknowns & require large computation time, many researchers such as Bortfeld (1961), Richards and Frasier (1976), Aki and Richards(1980) and Shuey (1985) obtained approximate solution of Zeppritz's equation by neglecting some terms and using some assumptions. AVO analysis requires seismic data to be processed by preserving relative amplitude during processing stage. Ostander (1984),



Chilburis (1984), Yu (1985) and Todd (1986) suggested several data processing work flows important for AVO study. AVO modeling / analysis comprises of three steps.

1. Detection of amplitude anomaly, AVO modeling using log derived rock properties and Aki-Richard's equation (1980) which is as follows.

$$R(\theta) = A + B \sin^2 \theta + C \sin^2 \theta \cdot \tan^2 \theta$$

where $R(\theta)$ is a model subsurface synthetic response which represents reflection coefficient with average angle of incidence θ . The constants used in the equations corresponds to

$$A = 1/2(\Delta V_p/V_p + \Delta \rho/\rho)$$

$$B = 1/2(\Delta V_p/V_p) - 2(V_s/V_p)^2 \times (\Delta V_s/V_s + \Delta \rho/\rho)$$

$$C = 1/2(\Delta V_p/V_p)$$

Where $\Delta V_p = V_{p2} - V_{p1}$, $\Delta \rho = \rho_2 - \rho_1$ and $\Delta V_s = V_{s2} - V_{s1}$ represent change in compressional velocity, density and shear velocity across interface from medium 2 to medium 1. Other terms used in the equation are

$$V_p = 1/2(V_{p1} + V_{p2}), V_s = 1/2(V_{s1} + V_{s2}) \text{ and } \rho = 1/2(\rho_1 + \rho_2)$$

which represent average compressional velocity, shear wave velocity and density across interface. V_{p1} , V_{s1} & ρ_1 and V_{p2} , V_{s2} & ρ_2 are compressional velocity, shear velocity and density of medium 1 and 2 respectively.

2. Creation of synthetic angle gathers based on model shear log / recorded shear log to confirm seismic anomaly

3. Lithological characterizations of the reservoir named as inversion of AVO data through cross-plotting of AVO attributes i.e. intercepts versus gradient, identifying data points showing anomaly from background trend and finally transposing this on intercepts section for marking areal extent of the anomaly.

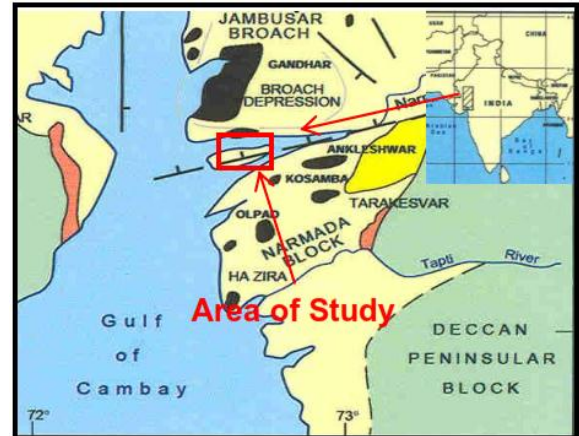


Fig- 1: Location map of study area.

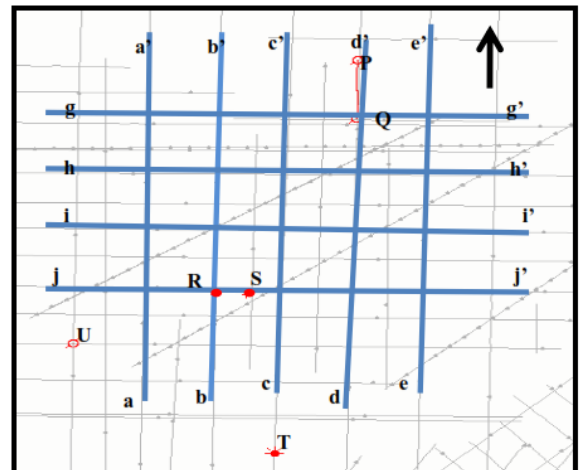


Fig-2: Map showing location of seismic lines and drilled wells. Part of seismic lines re-processed shown in blue color.

Present work

The present area of study is situated in the southern part of the Cambay Basin (Fig-1). Objective of present study is to analyze seismic data and Petrophysical properties of Hazad Formation of Middle to Late Eocene age. One of the most distinctive characteristics of the central part of study area is the presence of deltaic sedimentation and related complex coastal-interdeltaic system during the deposition of Hazad



AVO analysis in sandstone reservoir of Cambay basin.



Formation. The entrapment of hydrocarbons in is expected to be basically stratigraphic and / or strati-structural in nature.

The first well in the area was drilled in 1971 and was found to be oil bearing in Dadhar formation of Late Eocene to Oligocene age. This hydrocarbon discovery in the area has resulted in subsequent intensive exploration efforts by various operators such as British Gas, Canada's Hardy, Enron and Valco but of no avail.

2D seismic data was acquired in the area by Western Geophysical during 1985-1987 with hydrophones and marshy geophones using airgun / seiscord / dynamite as energy source, as the area extends from sea to transition zone to further on the land part too. This seismic data was processed by M/S Western Geophysical. Suitable amplitude / phase normalization / corrections were applied for hydrophone and marshy geophone data etc. Based on interpretation on this data, two wells i.e. P and Q were drilled in 2002 (Fig-2). The well P was abandoned without testing. However, it showed the presence of hydrocarbons in Hazad formation. The well Q was drilled at a distance of more than 2000m towards south of well P showed the presence of hydrocarbons in Hazad formation in Middle to Late Eocene age. However hydrocarbon presence was not commercial hence the well was abandoned. Subsequently ONGC drilled four more wells namely, T & U in the year 2010, R & S in the year 2011. Well U was dry and abandoned but well T showed influx of water with little oil. However, well R and S flowed gas and condensate from Hazad formation. Well S is an inclined well. In this paper results of AVO analysis / modeling are presented using log data of well R and seismic line b-b'.

Fig-2 above shows the location of 2D seismic lines in the area and drilled wells P, Q R, S, T and U. Seismic lines (shown by blue color) were reprocessed by preserving relative amplitude and Prestack migrated gathers were loaded on work station for AVO study. Fig-3 shows edited and resampled (2msec) sonic and density logs in track 1 &2 for the well R. It is observed that there is appreciable drop in density than sonic travel time in the reservoir zone. Petrophysical analysis was carried out for well R through

cross-plots in the depth interval of 1850-1920m representing Hazad formation which includes pay zone interval of 1889-98m.

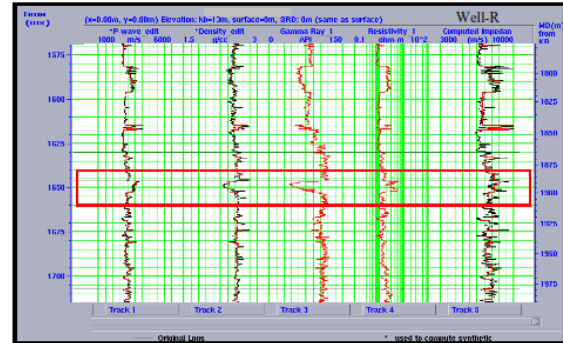


Fig-3: Edited Sonic and Density logs of well R (resampled at 2msec) in track 1 and 2. Zone of interest is marked with red rectangle.

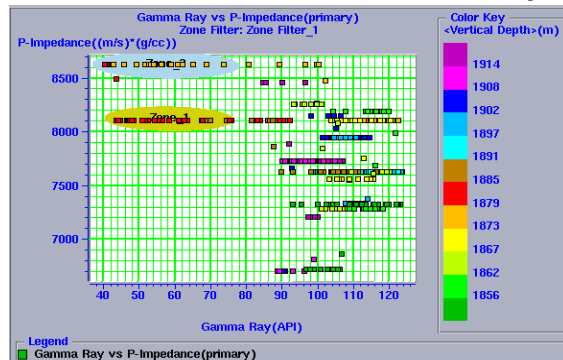


Fig-4a: Cross-plot GR versus computed impedance derived from sonic and density logs for the interval 1850-1920m for well R. Object in the interval 1889 -1898(1876- 85m TVD) flowed gas. Reservoir sand marked with light blue and yellow color has relatively high impedance compared to the shale above and below.

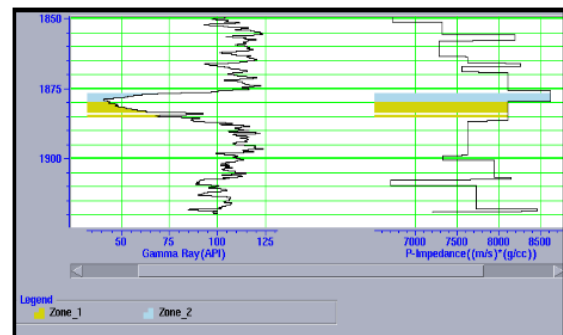


Fig-4b: Vertical cross-section of cross-plot of well R. Reservoir sands are of high impedance compared to nearby shale on top and bottom of pay.



AVO analysis in sandstone reservoir of Cambay basin.



"HYDERABAD 2012"

Cross-plot of GR versus computed Impedance (Fig-4a) indicates that the sandstone reservoir is of high impedance compared to the shale above and below it. High impedance sands are marked with yellow and light blue color elliptical boundary. Top part of the impedance section (blue zone) has relatively higher impedance than bottom part (yellow zone) as seen from vertical cross-section in Fig 4b. Shear log data is also recorded in this well which helped in understanding the response of modeled shear log created by Fluid Replacement modeling on the basis of log derived porosity and water saturation with actual recorded log and the gas response of synthetic gathers with PSTM gathers.

Cross-plot of V_p , compressional velocity versus V_s , shear velocity for the well R (Fig 5) shows drop in V_p in gas charged sediments from background i.e., shale / wet sand line which is expected in such gas charged reservoir. Log data of the well R processed on ELAN software using suitable parameters (Fig-6) shows cross over in RHOB and NPHI in the interval 1890-1898m. Effective porosity of the sand was 20% & average water saturation was found to be around 50% shown by blue line and light green colors respectively. AVO modeling was carried out on log derived V_p , V_s and RHOB parameters in the pay zone interval. Average values of V_p , V_s and ρ have been calculated from logs for top shale (3000, 1480 and 2.6), reservoir sand (3500, 2200 and 2.38) and bottom shale (3000, 1480 and 2.55) respectively. Aki-Richards equation was used to calculate the values of zero offset reflection coefficient represented by Intercepts 'A' (depends upon changes in density and P wave velocity) and gradient 'B' (depends upon density, P wave velocity and S wave changes) for top and bottom interfaces. Intercepts and gradient for top interface were found to be 0.032 and -0.37 and for the bottom interface 0.042 and 0.38 respectively. It is seen that reflection coefficient is marginally positive and gradient is

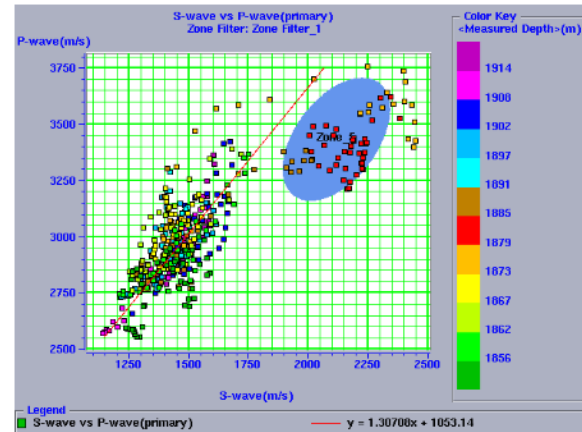


Fig-5: Cross-plot V_p versus V_s logs (well R) in the interval 1850-1920m. Data points from gas reservoir sands zone are marked with blue ellipse clearly showing separation from background trend of shale.

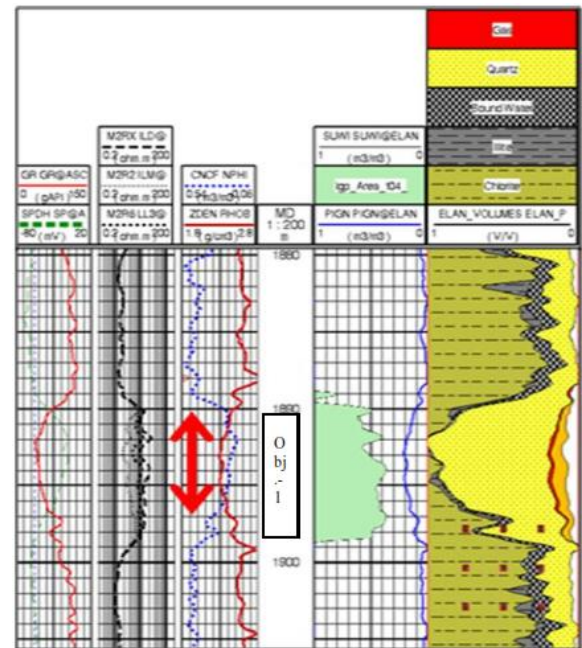


Fig-6 ELAN processed log data of well R for the Object-1 which produced gas at @ 77000m³ per day. Track -1 GR track -2 Resistivity and track-3 density and Neutron porosity log. Cross over is observed in Density and Neutron porosity log in the interval 1890-1896m marked with red arrow. Track-4 depicts water saturation in the zone 1890 to 1898.5 to be 50% and track 5 depicts quality of sand on the basis of volume of sand and shale. Gas bearing sand has effective porosity 20% and water saturation 50%.

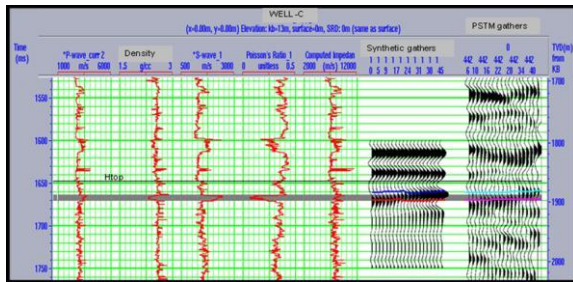


Fig -7 AVO Synthetic model for the In-situ, gas charged sand package to the left and the seismic gathers at well R to the right show phase reversal on far offset traces on the top of reservoir i.e., from Trough to Peak response classified as class II AVO anomaly. Density log shows drop in density due to gas effect but computed impedance is even higher for reservoir zone than background shale. Track 1 to 5 is Sonic, Density, Shear log, computed Poisson's ratio and Impedance log respectively.

highly negative for top interface and reverse is the case with bottom interface. This should theoretically result in a phase reversal at the far offset traces in a synthetic gather (Fig-7). The study has also indicated phase reversal at the far offset in PSTM gathers of the seismic line passing through the well R (Fig-7). On the basis of Rutherford and William (1989) classification this anomaly is class II AVO anomaly. Synthetic angle gathers were generated using AKI-Richards two term relation ($A+B*\sin^2\theta$) using 50% gas saturation and it is observed that synthetic gathers generated by modeled shear log by Fluid Replacement Model matches with insitu / recorded shear log thus validating the model.

Fig-7 shows correlation of synthetic angle gathers created using recorded shear log and wavelet extracted from seismic line b-b' passing through well-Rafter log correlation. As per present convention/definition, increase in impedance is represented by trough (negative number) on seismic trace. Therefore top interface from shale to sand would show phase reversal from trough to peak on far offset angle gathers and vice versa for bottom interface i.e. peak to trough for sand to shale. It is observed that synthetic angle gathers and PSTM angle gathers show good match and phase reversal as seen on far offset traces beyond 25 degree angle. Offset (distance) gathers were converted to angle gather by using velocity model

generated from well R. Hampson Russell software (Aki-Richards two terms equation) was used to create intercept and gradient volume on seismic line b-b'. Few seismic gathers near well-R (Fig-8) shows phase reversal on far offset. Normalized pick values of amplitude along the horizon near sand top (red) and sand bottom (blue) of the gas sand are displayed at the bottom of Fig-8. Sharp decrease in amplitude on far offset trace on PSTM gather is due to gas effect i.e., lowering of V_p / V_s ratio.

Intercept, Gradient analysis at CDP 442 & CDP 444 are shown in Fig-9 &10 of which left panel shows PSTM gathers, red and blue line indicating event pick near the top / bottom of the pay sand. Top right panel show amplitude versus offset variation near top and bottom of pay sand, red and blue lines showing estimation of intercept and gradient for respective CDPs, Correlation coefficient is 60%. Intercept is marginally negative and gradient is highly positive. Right bottom panel shows AVO analysis cross-plot intercept versus gradient from AVO inversion within the window of -10 to 40 msec and the location of intercepts and gradient for respective CDPs marked with red and blue dots for pay top and bottom. Data points of Gas charged zone show separation from background trend of shale / wet sand on the intercepts and gradient crossplot.

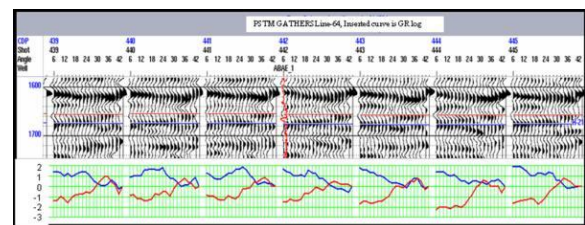


Fig-8 PSTM gathers of line b-b' near well R indicates phase reversal on far offset. Pick values of amplitude along the horizon near sand top (red) and sand bottom (blue) of the gas sand are displayed at the bottom.

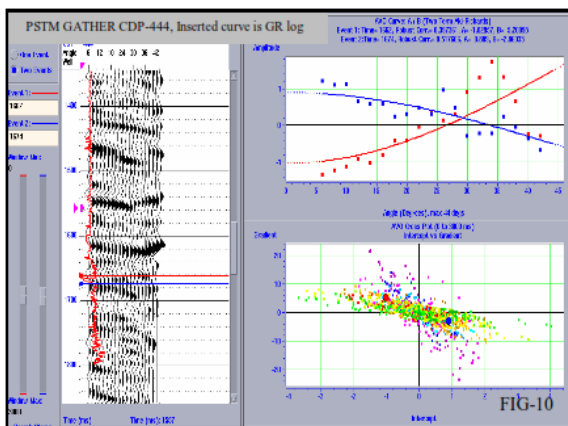
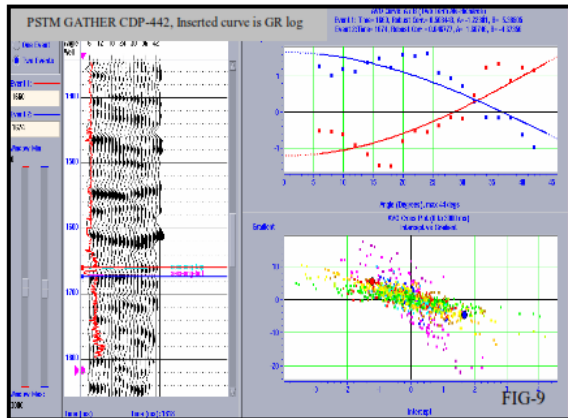


Fig-9 (top) & Fig-10 (bottom) show AVO analysis at CDP-442 and CDP-444 of the line b-near top and bottom of reservoir sand. Left panels are PSTM gathers with red and blue lines indicating event picks near the top and bottom of pay sand respectively. Top right panel showing amplitude versus offset variation near top and bottom of pay sand, red and blue lines showing estimation of intercept and gradient for respective CDPs, Correlation coefficient is 60%. Right bottom panel shows AVO analysis cross-plot intercept versus gradient from AVO inversion within the window of -10 to 40 msec and the location of intercepts and gradient for respective CDPs marked with red and blue dots for pay top and bottom.

Fig-11 is a cross plot of intercept versus gradient from AVO inversion of the seismic line **b-b'** with in the window of -10 to 40 msec from reservoir top. Regression line (red color) shows background trend of shale / wet sand. Yellow ellipse is drawn on the basis of intercepts and gradient observed near well R to identify location of AVO anomaly

on seismic line as a prospective area for hydrocarbon accumulation. Anomaly is marked by yellow ellipse superimposed on intercepts section to show areal distribution of AVO anomaly. Fig 12 shows presence of number of AVO anomalies on this line and their extension. Part of the seismic section is zoomed near the well to show extent of anomaly. AVO inversion has helped in identifying possible exploration target and deciding the drilling priorities on the basis of extent of the anomaly.

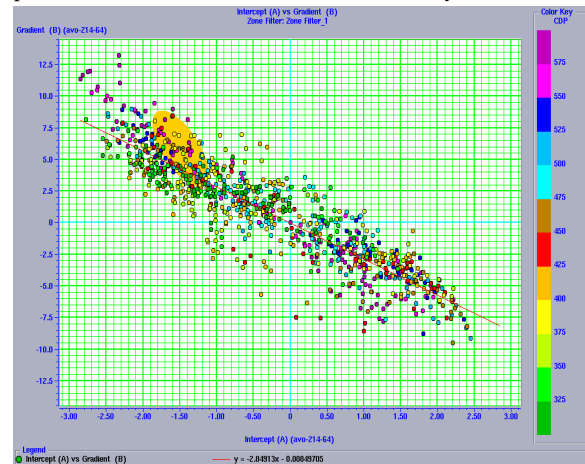


Fig-11 Intercept versus Gradient plot from AVO inversion of seismic line passing through well-R with in -10 to 40 msec window from reservoir top. Regression line (red color) shows back ground trend of shale/wet sand. Yellow ellipse was drawn on the basis values of intercepts and gradient observed near well R which helped to identify the AVO anomalies on the seismic line b- b' as a prospective area for hydrocarbon accumulation.

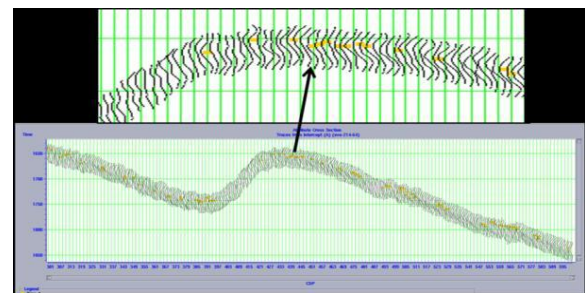


Fig-12 Intercept attribute derived from AVO inversion overlaid with AVO anomaly identified from the intercepts / gradient cross-plot. Zoomed part of the section placed on the top. AVO anomaly is observed at many places on this line which are possible hydrocarbon exploration leads.



Conclusions

- 1 Cross-plotting of rock properties indicate that reservoir sandstone is of high impedance encased with in low impedance shale. Large drop in Poisson's ratio for gas charged reservoir sand allow utilization of AVO technique to characterize the reservoir.
- 2 The AVO anomaly in the target zone in the present case has been classified as class II anomaly on the basis of marginally positive intercept and highly negative gradient computed from the model derived from log data. Synthetic gathers generated from the model show good correlation with real seismic PSTM gathers which show phase reversal at large offset for the gas charged.
- 3 Cross-plot of Intercept versus Gradient from AVO inversion shows marked separation of cluster of anomalous points from background trend (shale / wet sand) which has been identified as AVO anomaly. This AVO anomaly when overlaid on intercepts section has provided direct information about extension of possible gas reservoirs on the studied line.
4. AVO modeling / analysis has brought out number of AVO anomalies on the seismic line b-b' as possible exploration targets and will definitely prove helpful along with basic interpretation as the area is devoid of any 3-D data.

References

- Rutherford and Williams Amplitude versus offset variation in gas sands Geophysics vol 54, 1989.
- Yongyi Li, Jonathan Downton and Yong Xu Practical aspects of AVO modeling. The Leading Edge March 2007.
- John P Castagna, H.W.Swan and Douglas J Foster Framework for AVO gradient and intercept interpretation Geophysics vol 63 May-June 1998.

Mohamed A Eissa, John Pfeiffer and Heiman Alfredo Paz Ortega Seismic petrophysical analysis for thin sandstone reservoirs in Colombia's Guajira Basin. The Leading Edge June 2009.

Acknowledgments

The authors are thankful to ONGC for providing data and approval to publish this study. We also thank Shri P.B.Pandey, GGM-Basin Manager, WON for providing opportunity to work on this project and continuous guidance & encouragement.